Desalination and Water Treatment
www.deswater.com
doi:10.5004/dwt.2018.22677

123 (2018) 59–73
August

Production of sludge-based activated carbon: optimization and characterization

Muhammad H. Al-Malack*, Mohammed Dauda

Department of Civil and Environmental Engineering, King Fahd University of Petroleum and Minerals, Box 1150, Dhahran 31261, Saudi Arabia, Tel. +966138604735; Fax: +966138602789; emails: mhmalack@kfupm.edu.sa (M.H. Al-Malack), mohammeddauda18@gmail.com (M. Dauda)

Received 28 October 2017; Accepted 26 June 2018

ABSTRACT

Activated carbon (AC) was produced from sewage sludge using $ZnCl_2$, KOH, and H_3PO_4 as the activation agents. Effects of activation temperature (A), impregnation ratio (B), and activation time (C) on the yield and removal efficiency of methylene blue (MB) were investigated. Response surface methodology (RSM) and Box–Behnken design techniques and Design Expert software were used in the experimental design and optimization process. Based on the results, quadratic models for yield and MB removal efficiencies as functions of activation factors (A, B, and C) and their interactions were developed. When $ZnCl_2$ was used, the statistical analysis results clearly indicated that the yield model was statistically insignificant; however, B, AB, AC, and BC were significant. On the other hand, the MB model, AB, AC, A^2, A^2B, A^2C, and AB^2 were all found to be significant. Characterization of produced AC samples was limited to samples that produced higher values of yield and MB removal efficiency. At optimum conditions, the results showed that surface area and pore size of the produced AC were 319.5 m^2/g and 31.28 Å, respectively, which were obtained with $ZnCl_2$ at activation temperature and time of 700°C and 60 min, respectively, and impregnation ratio of 1:0.6. The Fourier transform infrared spectroscopy results clearly showed that dominant functional groups presented on the surfaces of produced AC samples were O–H, C–C, C–O, and C=O.

Keywords: Activation temperature; Activation time; Impregnation ratio; Yield; Methylene blue; Removal efficiency

1. Introduction

Activated carbon (AC) is a highly porous carbonaceous adsorbent with an extended particulate surface area that is made up of defective layers of graphene, which could appear in various configurations [1]. Moreover, Çeçen and Aktaş [2] described AC as being composed of microcrystallites that are made up of fused hexagonal rings of carbon atoms, which resemble graphite. AC is the most widely used adsorbent for various environmental decontamination, which is characterized by its high adsorptive capacity, high physiochemical stability, high surface reactivity, and an immense specific surface area (SSA) that can be as high as 2,000 m^2/g depending on production methods [3]. Its porous structure and particulate surface area allow it to adsorb and retain solutes and gaseous molecules. It is well known that any material with high lignocellulosic content (biomass) can be converted to AC via thermal treatment and activation [2].

Therefore, several materials such as coal, agricultural waste, household organic waste, and sewage sludge have been used in the production of AC [4–7]. Carbonization and activation are the main processes involved in the production of AC, which can be performed individually in two consecutive steps or in one single step. Pullket [1] defined carbonization as the thermal conversion of organic materials into its consolidated form of carbon, whilst eliminating noncarbon elements under an inert atmosphere. Chars are produced through aromatization and polymerization reactions of carbonaceous materials at high temperatures [1]. Parameters that affect yield and characteristics of produced chars during carbonization process include carbonization temperature, activation time, heating rate, and the nature of precursors used.

* Corresponding author.

Produced chars are activated through either physical or chemical activation methods, where activation process is normally carried out to create more pore structures and extended surface area within the char/carbonaceous sample to enhance its adsorptive capacity. Physical activation is achieved through the gasification of carbonized chars with a gas (oxidant), such as steam, carbon dioxide, oxygen, and air, at high temperatures (600°C–900°C) to further aid in porosity development [8]. In chemical activation, carbonization and activation are usually performed simultaneously, however, the two-step approach has also been reported, where produced chars are impregnated with a chemical reagent (oxidant) such as, KOH, $ZnCl_2$, H_3PO_4, H_2SO_4, and NaOH. Subsequently, produced slurries are subjected to another round of carbonization. In the one-step approach, carbonaceous precursors are impregnated with a chemical reagent and the produced mixture is carbonized at high temperatures that are sufficient for pyrolytic reactions to take place [8]. The impregnation process supports the pyrolytic decomposition of organics present in the precursor, limits tarry residue formation in the pores, and assists in preventing pores blockage [1].

The three most commonly used activating chemicals are $ZnCl_2$, KOH, and H_3PO_4, which have various reaction mechanisms with carbonaceous precursors during activation. $ZnCl_2$ is reported to act as a dehydrating agent in the early stage of carbonization, which results in charring and aromatization that, subsequently, leads to the formation of pore structures. In KOH activation, potassium reacts with precursors, which results in the formation of intercalation compounds (potassium compounds) that infiltrate into the carbon network causing accelerated carbon loss and pore development. With respect to H_3PO_4, its chemical interaction with carbonaceous precursors usually results in porosity development by its intercalation in the internal structure of precursors [9]. Acid, alkaline, or distilled water are used to wash produced AC in order to remove residuals of activating reagents and to free blocked pores [10].

AC derived from sewage sludge is commonly referred to as sludge-based adsorbent (SBA), where Kemmer et al. [11] were the first to patent the art of AC production from dried sewage sludge using chemical activation. Hadi et al. [12] and Smith et al. [8] have both published detailed literature reviews on production of AC from sewage sludge, where they covered production processes, AC properties and their applications in removal of contaminants from water and wastewater. The two reviews concluded that AC produced from sewage sludge by chemical activation methods exhibited considerable high surface properties than those produced by physical activation methods. Moreover, they reported that adsorption capabilities for various pollutants is influenced mainly by the produced AC surface area and surface functional groups that are known to be responsible for uptake of contaminants. Furthermore, high surface areas of ACs have been produced from sewage sludge in the past few years by several researchers, who employed different activation methods. Wang et al. [13] produced a highly porous AC from recycled activated sludge sample collected from a secondary precipitator of municipal wastewater treatment plant. They reported that sludge was activated using 3.0 M KOH at an activation temperature and time of 600°C and 60 min, respectively. The results showed a specific Brunauer–Emmett–Teller (BET) surface area of 382 m^2/g was achieved. Adsorption of acid brilliant scarlet (GR) dye was investigated using the produced AC and the results showed that 99.6% and 99.7% of total organic carbon and color, respectively, were removed from the aqueous solution containing the dye. Wen et al. [14] investigated the production of AC from sewage sludge that was used for the adsorption of gaseous formaldehyde. The AC was produced through chemical activation of sewage sludge using 6.0 M $ZnCl_2$ in the presence of nitrogen gas at an activation temperature and time of 750°C and 120 min, respectively. The investigators reported that the activation process produced AC with a BET surface area of 509.88 m^2/g. Furthermore, the produced AC was compared with some commercial activated carbons (CAC) in the adsorption of gaseous formaldehyde. They reported that the produced AC was found to exhibit an excellent adsorption capacity that is higher than that of CAC samples. They attributed the results to its porous structure and appropriate surface chemistry that favored the adsorption of gaseous formaldehyde. Alvarez et al. [15] investigated the effect of HCl and Na_2CO_3 washing of pyrolyzed sewage sludge char on its activation with CO_2 at an activation temperature of 800°C in a fixed bed reactor. They found that the washing step contributed immensely to the produced char gasification rate, which also further assisted in improving the produced AC properties. They reported that a BET surface area of 440 m^2/g was achieved for the produced AC for an activation time of 15 min.

Based on the earlier discussion, the main objective of the current investigation is to study the effect of activation parameters such as activation temperature and time and impregnation ratio on the yield and removal efficiency of methylene blue (MB) of produced AC samples, where a quadratic model will be formulated using the Box–Behnken design (BBD) and response surface methodology (RSM) techniques and Design Expert software. Moreover, characterization of raw sludge and selected produced AC samples is the second main objective of the investigation, where characterization will include parameters such as elemental analysis, thermogravimetric analysis (TGA), X-ray powdered diffraction (XRD), X-ray fluorescence (XRF), Fourier transform infrared spectroscopy (FTIR), scanning electron microscopy (SEM), and BET surface area. It is worth to mention that up to the knowledge of the authors, the current research is the first of its kind in the Kingdom of Saudi Arabia.

2. Materials and methods

2.1. Materials

Dewatered sewage sludge sample was collected from Al-Khobar wastewater treatment plant in the Eastern Province of Saudi Arabia. The general characteristics of the collected sludge samples can be cited in Al-Malack et al. [16]. It is worth to mention that the only treatment, which was given to the utilized sludge, was dewatering on sand drying beds or mechanical filter presses. The collected sludge was oven dried at 105°C, washed and redried again. The final product was comminuted, sieved through a 2-mm sieve size and stored in covered plastic containers. All chemical reagents

that were used in the current investigation such as cadmium nitrate salt, phenol crystal, MB, potassium hydroxide pellets, phosphoric acid solution, zinc chloride, and nitric acid were of analytical grade.

2.2. Experimental design

Prior to activation, dried sludge was characterized for its ash content, elemental analysis, and TGA. Subsequently, AC was produced from the dried sludge using three activating chemical reagents, namely zinc chloride ($ZnCl_2$), potassium hydroxide (KOH), and phosphoric acid (H_3PO_4). The BBD and RSM techniques were utilized during the production process, where three levels were selected for each independent factor (activation temperature, impregnation ratio, and activation time) that may affect the production process. The significance of each of the factors, under investigation, was assessed based on the yields and MB removal efficiencies of the produced AC samples. The selected levels for each factor were coded as low (−1), medium (0), and high (+1), as shown in Table 1. A total number of 13 experimental runs were created for each activating agent, with one replicated center run per block. The BBD design was selected for the activation process because it offers fewer experimental runs, when compared with other RSM designs, and allows efficient estimation of first- and second-order coefficients of resulting mathematical models by considering the corner points of a three-level factorial design [17]. Mathematical models based on polynomial equations that describe the effect of each individual factor on the responses (yield and MB removal efficiency) were generated from experimental designs. The mathematical response model developed was in the following form:

$$y = \beta_o + \sum_{i=1}^{k} \beta_i x_i + \sum_{i=1}^{k} \beta_{ii} x_i^2 + \sum_{i=1}^{k-1} \sum_{J=2}^{k} \beta_{ij} x_i x_j + \varepsilon$$

where y is the predicted response, β_o is a constant term coefficient, β_i is a linear term, β_{ii} is a quadratic term, β_{ij} is an interaction term, ε is an error term, and $x_i x_j$ is the coded values of the independent variables. The experimental design and the subsequent statistical analyses of the two responses that were obtained from each activation process were achieved and aided by a statistical software called Design Expert (version 9).

Table 1
Factor levels and coding for activation agents

Factor	Unit	Agent	Symbol	Coded factors		
				−1	0	1
Temperature	°C	$ZnCl_2$	*A*	600	700	800
	°C	KOH	*B*	600	700	800
	°C	H_3PO_4	*C*	600	700	800
Impregnation ratio	Ratio	$ZnCl_2$	*A*	0.2	0.6	1
	Ratio	KOH	*B*	0.5	1	1.5
	%	H_3PO_4	*C*	30	40	50
Activation time	Min	$ZnCl_2$	*A*	60	90	120
	Min	KOH	*B*	60	90	120
	Min	H_3PO_4	*C*	60	90	120

2.3. Production of activated carbon

During the impregnation stage of $ZnCl_2$ and H_3PO_4, 10 g of the dried sludge were mixed and stirred with 15 mL solution of the activating reagents, as per the experimental design, to achieve the desired impregnation ratio. With respect to KOH impregnation, 10 g of the sludge were mixed with varying weights of crushed KOH pellets, as per the experimental design, until homogenous mixtures were attained. The impregnation process was performed at room temperature and the activating agents were kept in contact with the sludge for more than 1 h to achieve full penetration, subsequently, the obtained slurry was oven dried at 105°C for 4 h to remove excess moisture. The impregnated samples were then packed into 30 cm long stainless steel tubes of 50 mm diameter having two narrow ports of 8 mm diameter (for expelling gases). The tubes were placed in a muffle furnace and heated to the desired temperatures of 600°C, 700°C, and 800°C. The furnace was heated slowly at 10°C/min until targeted temperatures were reached, afterwards, samples were taken out of the furnace at time intervals of 60, 90, and 120 min. Obtained AC samples were cooled and subjected to repeated cycles of washing with distilled water until pH of the wash water reached values of 6–7. The final products were oven dried at 105°C for 24 h, crushed, and sieved to particle sizes of less than 0.3 mm.

2.4. Characterization of sludge and produced AC

The best obtained AC samples, in terms of yield and MB removal efficiency, were characterized using scanning electron microscopy coupled with energy dispersive X-ray spectroscopy (SEM/EDS), XRD, XRF, TGA, FTIR, elemental analysis and porosity, and surface area analyzer for determining the BET surface areas and pore volumes.

2.4.1. Thermogravimetric analysis

TGA measures the effect of temperature increase on weight change of a material, which primarily measures the oxidative and decomposition stability of the material with respect to temperature changes. In the current research, TGA was carried out to investigate thermal responses of sludge and selected produced AC samples when pyrolyzed in an argon gas atmosphere. An approximate weight of 20–35 mg of samples was placed in an alumina crucible and loaded onto the device. Another crucible containing Al_2O_3, used as a reference for differential scanning calorimetry measurement, was also loaded. Samples were pyrolyzed at a heating rate of 10°C/min, starting from a temperature of 30°C to 1,000°C, under an argon gas flow rate of 100 mL/min.

2.4.2. Ash content analysis

Total ash content of the sludge was determined according to the ASTM D2866-94 test method. The procedure involved igniting a clean ceramic crucible in a muffle furnace at a temperature of 650°C for 1 h, cooled in a desiccator and

weighed. Subsequently, about 2 g of sludge were weighed and heated to a temperature of 650°C until no weight change was recorded.

2.4.3. Elemental analysis (CHNS-O)

The organic elemental composition of sludge and produced AC samples was determined using the CHNS/O Elemental Analyzer (PerkinElmer, USA). Carbon, hydrogen, nitrogen, and sulfur content of samples were derived from their combustion analysis.

2.4.4. Surface morphology

Surface shapes and pore structures of sludge and produced AC samples were determined by their magnified images through SEM (JSM-6610LV) coupled with energy dispersive X-ray spectrometer (EDS). The EDS was used to identify the surface elemental compositions of each sample during SEM scans. An accelerating voltage of 20 kV was employed for the SEM scans, where three scan resolutions were undertaken for each sample (10, 50, and 100 μm).

2.4.5. Powdered X-ray diffraction spectroscopy

Mineralogical compositions of sludge and produced AC samples were carried out using the XRD technique. The XRD analysis provides information on crystalline inorganic compounds present in a sample, through the study of its X-ray diffraction patterns. Rigaku Ultimate IV X-ray Diffractometer using copper K-α radiation was used for the XRD analysis, where diffraction patterns were obtained by scanning at 0.02°/s step size with an angle ranging from 10° to 80°.

2.4.6. X-RF spectroscopy

The XRF analysis was conducted for sludge and produced AC samples using Spectro Xepos equipment (Ametex, USA), which was conducted to determine and quantify inorganic compounds. The XRF is also an elemental analysis that is based on the emission of characteristic X-ray radiation by a material bombarded with either X-ray or gamma photons [18].

2.4.7. FTIR spectroscopy

Identification of functional groups on surfaces of sludge and produced AC samples was achieved using the FTIR technique using Thermo Electron Corporation Nicolet Nexus 670 FT-IR Spectrometer at wavelength region of 500–4,000 cm^{-1}, where potassium bromide (KBr) method was used. Prior to analysis, samples were homogenously mixed and ground with KBr (spectroscopy grade) in a mortar and, subsequently, pressed hydraulically to form pellets, which were then transferred to the FTIR spectroscopy.

2.4.8. Porosity and surface area

Porosity characterization of sludge and produced AC samples was achieved using an automatic physio-sorption unit (Micrometric, ASAP 2020, USA). SSA_{BET}, pore volume, and pore size were determined through the classical BET theory and the nitrogen adsorption/desorption isotherm data at 77°K.

2.4.9. Yield and methylene blue adsorption

Yield is the percentage of mass final produced ACs to the mass of sludge used in the activation process. Yields of produced AC were determined and used in the optimization of the production factors. MB adsorption experiments were investigated for produced AC samples. This was done to provide an experimental response required for the optimization of the production factors. Also, the selection of best produced AC samples for characterization was performed based on their MB removal efficiency. The MB adsorption experiments were performed as follows, about 0.1°g of produced AC was combined with 50 mL volume of 100 or 20 mg/L MB solution in an Erlenmeyer flask. The flask was agitated using a mechanical shaker at 200 rpm for a predetermined time. The resulting solution was, subsequently, centrifuged and the supernatant was analyzed using UV spectrophotometer (Shimadzu 1650).

3. Results and discussion

3.1. Statistical analysis and modeling

Table 2 shows the complete experimental design layout together with the obtained responses for each $ZnCl_2$, where activation temperature, impregnation ratio, and activation time were designated as *A*, *B*, and *C*, respectively. Similar results were obtained for the other two activation agents (KOH and H_3PO_4). Data analyses were automatically carried out using the Design Expert V.9.0 software, which employs the least square regression method in fitting the experimental data to the selected polynomial function. Response transformation was performed as needed on some of the responses in order to satisfy the normal distribution criteria. Different model types suggested by the software for both responses (yield and MB removal efficiency) were refined by adjusting some of their terms to ensure that the model terms were not biased. Derived empirical models for each activating agent are presented below, where *Y*, MB, *A*, *B*, and *C* are yield, MB removal efficiency, activation temperature, impregnation ratio, and activation time, respectively.

3.1.1. $ZnCl_2$ activation

$$\frac{1}{Y} = 0.018 + 6.526\times10^{-4}A - 1.672\times10^{-3}B + 1.403\times10^{-4}C + 7.287\times10^{-4}AB + 8.319\times10^{-4}AC - 9.739\times10^{-4}BC + 6.074\times10^{-4}A^2 - 1.833\times10^{-4}C^2 + 5.854\times10^{-5}A^2B + 5.949\times10^{-4}A^2C - 4.977\times10^{-4}AB^2$$

$$\frac{1}{\mathrm{MB}} = 0.017 + 1.456\times10^{-3}A - 0.16B + 2.587\times10^{-3}C + 7.393\times10^{-3}AB + 1.709\times10^{-3}AC - 3.366\times10^{-3}BC - 4.927\times10^{-3}A^2 + 9.088\times10^{-3}B^2 + 4.989\times10^{-3}A^2B - 8.790\times10^{-3}AB^2$$

Table 2
Experiment design and response results for $ZnCl_2$ activation

Run	Factor 1	Factor 2	Factor 3	Response 1	Response 2
	A: Temperature	*B*: Impregnation ratio	*C*: Time	Yield	MB removal
	(°C)	(Sludge: $ZnCl_2$)	(min)	(%)	(%)
1	800	1:0.6	60	56.5	96.3
2	700	1:1	60	58.4	97.9
3	600	1:0.6	60	55.4	91.825
4	700	1:0.2	120	48.2	20.3
5	600	1:1	90	59.6	97.8
6	700	1:1	120	64.7	96.225
7	700	1:0.2	60	54	28.075
8	600	1:0.2	90	49	21.2
9	800	1:1	90	53.9	96.6875
10	800	1:0.6	120	48	58
11	800	1:0.2	90	51.9	56.45
12	700	1:0.6	90	54.8	58.55
13	600	0.6	120	56	91.65

3.1.2. KOH activation

$$\sqrt{Y} = 4.99 - 0.09A - 0.24B - 0.25C + 0.62AB + 0.23A^2 - 0.43C^2 - 0.32A^2B - 0.85AB^2$$

$$\sqrt{MB} = 9.72 + 0.28A + 0.34B + 0.065C - 0.17AB - 0.11AC + 0.019BC - 0.27A^2 - 0.19A^2B - 0.32A^2C - 0.20AB^2$$

3.1.3. H_3PO_4 activation

$$Y = 59.46 - 4.13A - 6.42B - 1.13C - 1.03AB - 3.76A^2 + 2.00A^2B - 1.3AB^2$$

$$\mathrm{MB} = 82.84 - 39.08A + 10.65B - 2.54C + 3.08AB - 26.4A^2 + 4.26A^2C + 11.59AB^2$$

Table 3 shows a comparison between observed and predicted responses based on the derived empirical models, when $ZnCl_2$ was used as the activating agent. The results showed that the predicted yields and MB removal efficiencies for each activation process were in good agreement with the observed responses. Correlation coefficient values (R^2) of the models, as shown in Table 4, were all close to unity, which support the reliability of the models. As part of the conditions for model adequacy, adjusted and predicted R^2 values need to be in agreement, and this can only occur whenever their difference is less than or equal to 0.2. The observed differences for the yield and MB removal efficiency models were 0.1304 and 0.0812, respectively. The adequate precision value of a model measures the signal-to-noise ratio and a value greater than 4 is desirable for a model to adequately predict the experimental data within the design space [19]. Adequate precision values of 50.60 and 24.258 achieved for the two models showed that they are both of adequate signals. The average absolute deviation (AAD) value indicates the predictive capability of the developed models and highly reliable models usually present low AAD value. AAD values of 0.1388% and 4.8195% were achieved for the two models, respectively. Similar results and conclusions were obtained when other activation agents (KOH and H_3PO_4) were used. Results of analysis of variance, which was performed at 5% (0.05) level of significance on the models, are presented in Table 5. The table shows the significance level of each model and its terms based on the probability value (*p*-value) and the *F*-statistic value. A *p*-value < *F* < 0.050 indicates that the model or the term is statistically significant in predicting the experimental response; otherwise, it denotes that the term or the model is statistically insignificant. Focusing on the $ZnCl_2$ activation process, the yield model presented a *p*-value of 0.0517, which is greater than 0.05 and, therefore, implies that the model is not significant. The significant model terms were found to be *B*, *AB*, *AC*, and *BC*, as their *p*-value were all less than 0.05. With respect to the MB removal efficiency model, the model itself and the following terms, *AB*, *AC*, A^2, A^2B, A^2C, and AB^2 were all statistically significant. Based on this outcome, it was concluded that for the two developed models, both temperature (*A*) and activation time (*C*), had no significant effect on the yield of the AC samples produced by $ZnCl_2$ activation, but impregnation ratio (*B*) and various cross-product contribution (interaction term) of each factor showed significant effects on the yield. On the other hand, the MB removal efficiency model showed that all single model terms, namely activation temperature (*A*), impregnation ratio (*B*), and activation time (*C*) were having significant effects on the MB removal efficiency of the produced AC samples, while some of the interaction terms were found to be insignificant. Table 5 shows the results of statistical analyses that were performed for KOH and H_3PO_4.

3.2. Response surface plots

Three-dimensional (3-D) response surface and contour plots of measured yields and MB removal efficiencies for the

Table 3
Responses predictions for all activation agents based on developed models

$ZnCl_2$ activation				KOH activation				H_3PO_4 activation			
Yields (%)		MB removal (%)		Yields (%)		MB removal (%)		Yields (%)		MB removal (%)	
Actual	Predicted	Actual	Predicted	Actual	Predicted	Actual	Predicted	Actual	Predicted	Actual	Predicted
56.5	57.10	96.3	108.31	19.6	19.78	83.15	79.98	57.1	54.17	92.65	96.03
58.4	58.90	97.9	92.02	18.4	16.56	96.78	96.79	54.2	59.46	80.13	82.84
55.4	55.97	91.83	102.68	19.5	21.46	86.15	89.25	65	64.52	75.88	76.72
48.2	48.54	20.3	20.82	24.7	24.90	94.70	94.48	56.2	55.72	14.75	15.58
59.6	60.12	97.8	97.36	32.3	30.69	92.63	89.61	59.4	60.96	91.55	94.16
64.7	65.31	96.23	107.42	21.6	22.81	92.10	89.00	66.8	64.75	69.68	69.65
54	54.42	28.08	27.67	24.7	24.48	97.10	100.26	52.4	52.7	15.45	16
49	49.35	21.2	21.24	20.9	20.70	94.70	94.71	49.8	50.44	16.85	19.44
53.9	54.32	96.69	99.71	28.6	26.34	91.75	88.30	51.6	51.91	92.30	90.95
48	48.43	58	56.10	25.3	25.50	92.90	92.93	58.2	57.74	94.40	91.86
51.9	52.29	56.45	57.92	44.3	46.02	92.15	95.61	45.3	44.82	45.60	43.04
54.8	55.56	58.55	58.82	15.4	14.29	80.05	83.21	67.6	67.01	79.48	74.73
56	56.59	91.65	86.99	19.1	20.88	93.50	93.51	59.3	58.7	97.05	97.6

Table 4
Important characteristics of models

Agent	Response %	Response	Adeq. precision	R^2	Adj. R^2	Pred. R^2	AAD %
$ZnCl_2$	Yield	Inverse	50.60	0.9996	0.9952	0.8648	0.1388
	MB	Inverse	24.26	0.9976	0.9854	0.9042	4.8195
KOH	Yield	Square root	15.33	0.9701	0.9104	0.8119	3.239
	MB	Square root	53.62	0.9993	0.9956	0.9511	0.1374
H_3PO_4	Yield	None	9.42	0.9153	0.7966	0.6478	2.1785
	MB	None	27.81	0.9943	0.9862	0.9546	3.4637

Table 5
Analysis of variance at 5% ($p < 0.05$) level of significance for developed model

Agent	Response %	Model	A	B	C	AB	AC	BC	A^2	B^2	C^2	A^2B	A^2C	AB^2
$ZnCl_2$	Yield	0.0517	0.053	0.0211	0.237	0.048	0.042	0.036	0.069		0.219	0.084	0.083	0.099
	MB R	0.0121	0.237	0.003	0.052	0.014	0.189	0.061	0.042	0.013		0.056		0.019
KOH	Yield	0.0084	0.440	0.093	0.029	0.592			0.141		0.029	0.281		0.005
	MB R	0.0036	0.090	0.063	0.019	0.003	0.007	0.174	0.001			0.005	0.002	0.004
H_3PO_4	Yield	0.0194	0.040	0.008	0.338	0.525			0.080			0.390		0.567
	MB	<0.0001	<0.001	0.001	0.235	0.162			<0.001				0.170	0.007

three activation agents were developed in order to visualize and discern effects of each factor (activation temperature, impregnation ratio, and activation time) on the two observed experimental responses (yield and MB removal efficiency). It should be noted that some of the plots displayed the two interaction factors that were significant to the response only.

3.2.1. Effect of production factors on yield

Fig. 1 presents the 3-D response surface and contour plots showing effects of activation temperature, impregnation ratio, activation time, and their interactions on yields of AC samples produced by $ZnCl_2$, as the activation agent. The Fig. 1 clearly shows that the impregnation ratio seems to have a more pronounced effect on the yields of the AC samples than activation temperatures and times. Moreover, the figure shows that an increase in impregnation ratio from 0.2 to 1 showed a favorable rise in the yield up to a maximum value of 64.5%. This implies that the concentration of $ZnCl_2$ employed, during the activation process had greater influence on the outcome of yields than other factors. These results are in total agreement with those reported by Ucar et al. [20] in their research

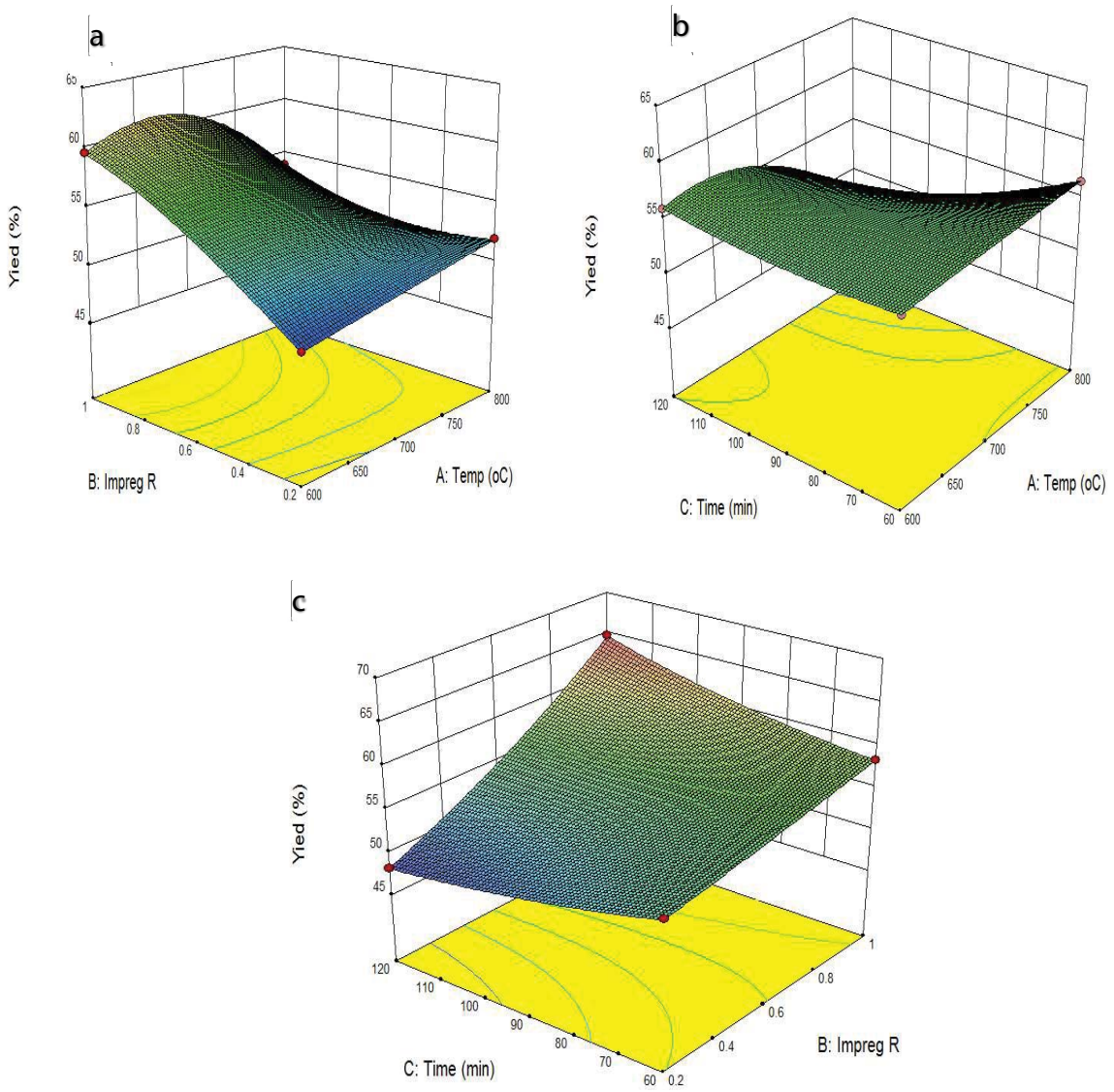

Fig. 1. 3-D surface plot of yield of AC produced by $ZnCl_2$. (a) Yield (%) versus impreg R and temp (°C); (b) yield (%) versus time and temp (°C); and (c) yield (%) versus time and impreg R.

work on AC production from pomegranate seed, where they observed that the concentration of $ZnCl_2$ had an effect on the yield of produced AC samples. Moreover, the interaction effects of the temperature–impregnation ratio (Fig. 1(a)) and temperature–time (Fig. 1(b)) were both found to have antagonistic effects on the obtained yields, while the interaction of temperature–impregnation ratio (Fig. 1(c)) shows favorable effects for the conditions studied. When KOH was used as the activation agent, the results showed that the interaction of temperature with impregnation ratio had negative impacts on yields of the produced AC samples. The results showed that at lowest levels of temperature and impregnation ratio, high yield of 44% was obtained, however, as temperatures and impregnation ratios were increased, sharp drops in the response were observed. This outcome was found to be in agreement with the statistical analysis results presented for KOH activation that were shown earlier. The influence of these factors on the yield can be attributed to the increase rate of gasification reactions (devolatilization) that occurs at higher temperatures during carbonization and to the reaction mechanism of KOH with the carbonaceous precursor that can lead to high carbon loss during development of pores [21]. Some researchers reported that, in the course of pore development in KOH activation, intercalation compounds (K_2O and others) formed at high temperatures can penetrate carbon networks and result in high carbon loss during volatilization [6,22]. The range of yields recorded for KOH activation was quite low for the selected experimental conditions, which was around 15%–45%, however, this was found to be in agreement with results reported on AC production with KOH activation [6,23]. Similarly, when H_3PO_4 was used as the activation agent, the results showed that the interaction of activation temperature and H_3PO_4 concentration had negative impacts on the yield of the produced AC, where increase in activation temperatures and H_3PO_4 concentrations resulted in slight decreases in yield percentages.

3.2.2. Effect of production factors on MB removal efficiency

Fig. 2 presents 3-D response surface and contour plots, which shows effects of activation temperature, impregnation ratio, activation time, and their interactions on MB removal efficiency of the produced AC when $ZnCl_2$ was used as the activating agent. The figure clearly shows that the impregnation ratio had more significant impacts on the results of MB removal efficiencies than other factors, where a decrease in MB removal efficiency from 97% to 20% was noticed when the impregnation ratio was decreased from 1 to 0.2. The results can be better explained by noting that at higher impregnation ratios, the possibility of developing more pores according to the reaction mechanism of $ZnCl_2$ with the precursor is more likely to occur than at lower ratios during the activation process. Zhang et al. [24], who produced AC from sewage sludge reported that the use of high $ZnCl_2$ concentration, during activation process, was found to result in its deposition on the external structure of the carbon particles. Consequently, the deposition of $ZnCl_2$ may have resulted in the decomposition of organic matter in its close vicinity and, therefore, contributed in creating more porous structures and, consequently, high MB removal efficiencies recorded for high impregnation ratios are justifiable. With respect to KOH, the results showed that activation temperature was found the be the dominant factor affecting MB removal efficiencies, where high MB removal efficiencies were observed at high temperature values and low removal efficiencies were obtained at low activation temperatures. This outcome might have resulted from the effect of high temperatures on the activation process that led to increased rates of reaction between sludge and reagents, during the activation process, which resulted in the formation of more pore structures. Several researchers have also reported the implication of high activation temperatures on adsorption properties of produced AC samples. Utomo et al. [25], who investigated MB adsorption

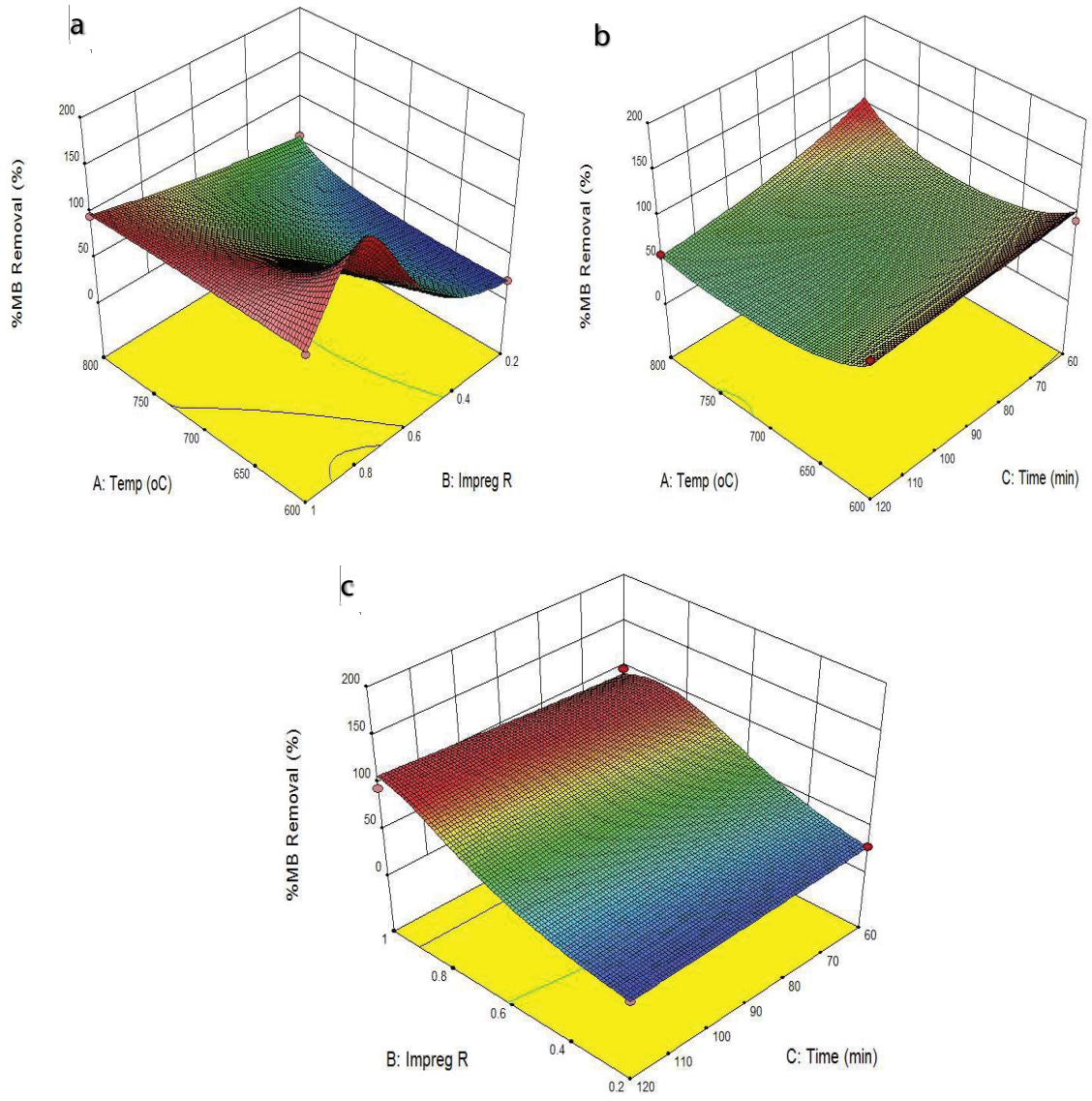

Fig. 2. 3-D surface plot of MB removal efficiency of AC produced by $ZnCl_2$. (a) %MB removal versus impreg R and temp (°C); (b) %MB removal versus time and temp (°C); and (c) % MB removal versus time and impreg R.

using biochar (nonactivated) derived from sewage sludge, reported that sludge samples heated at high temperatures showed high MB removal efficiencies, where a maximum removal efficiency of 95% was reported for sludge samples that were heated at 700°C for 2 h. Similarly, when H_3PO_4 was used as the activation agent, the results showed that the influence of temperature on MB removal efficiencies for all samples was quite significant, when compared with other factors. An increase in temperature from 600°C to 800°C resulted in a decrease in MB removal efficiency to its lowest value of 15%, which can be attributed to the effect of high temperatures as described in the case of KOH activation.

3.3. Characterization of sludge and produced AC

Produced AC samples that generated relatively high yields and MB removal efficiencies were subjected to another round of MB adsorption experiment, where higher concentration of MB (100 mg/L) was used. Samples that produced best results in the adsorption of MB were selected for the characterization process. Accordingly, two AC samples were selected from $ZnCl_2$ activation process (AC1-$ZnCl_2$ and AC2-$ZnCl_2$) and one from KOH activation process (AC3-KOH). Sample AC1-$ZnCl_2$ was activated at a temperature of 700°C, impregnation ratio of 1:1 (10 g sludge with 15 mL of 5.0 M $ZnCl_2$ solution), and activation time of 120 min, while AC2-$ZnCl_2$ was activated at same conditions of temperature and impregnation ratio and activation time of 60 min. On the other hand, AC3-KOH was activated at temperature of 700°C, impregnation ratio of 1:1.5, and activation time of 60 min. The three selected samples were subjected to various investigations to determine their surface properties, pore structures, and elemental compositions.

3.3.1. Elemental analysis

Table 6 shows elemental analysis of the three AC samples together with the raw sludge. When comparing carbon contents of the raw sludge with those of the produced AC samples, a remarkable decrease can be observed, which might have resulted from initial volatilization of organics at lower temperatures of the pyrolysis stage and carbon burn-off at higher temperatures [1]. Low nitrogen contents in AC samples (<3%) could indicate that the majority of functional groups are oxygen-based [26]. The increase in carbon–hydrogen (C/H) ratios of AC samples in comparison with that of the raw sludge implies an increase in the aromatization of the carbon structure, which resulted from the activation process. The table clearly shows that the increase in C/H ratios was of the following order: AC1-$ZnCl_2$ < AC2-$ZnCl_2$ < AC3-KOH.

Table 6
Elemental composition of sludge and produced AC samples

Parameters	AC1-$ZnCl_2$	AC2-$ZnCl_2$	AC3-KOH	Sludge
C (%)	22.14	22.91	14.36	38.24
H (%)	1.05	1.35	1.11	5.17
N (%)	2.02	2.27	1.33	5.80
S (%)	1.24	1.19	0.12	1.33
Others (%)	73.55	72.28	83.08	49.46
C/H	21.09	16.97	12.94	7.40

3.3.2. Thermogravimetric analysis

Combined thermogravimetric (TG) and derivative thermogravimetric (DTG) curves of sludge and produced AC samples are presented in Fig. 3. Figs. 3(a) and (b), which belong to samples activated with $ZnCl_2$, indicate that both samples exhibited three stages of weight loss in response to temperature increase. The first stage, which occurs between 30°C and 100°C, accounts for about 7% of weight loss and was attributed to the release of moisture from AC samples. A negligible weight loss of approximately 4% can be noticed between 100°C and 725°C, while more pronounced weight loss of approximately 22% was recorded between 725°C and 1,000°C. The last two stages can be attributed to decomposition and volatilization of fused $ZnCl_2$ or ZnO and other inorganic constituents in the carbon structure that resulted from the activation process [27]. Fig. 3(c), which belongs to sample activated with KOH, shows that two stages of weight loss took place during the activation process. The figure clearly shows that in a temperature range between 30°C and 150°C, an abrupt weight loss of approximately 9% was observed, which can be attributed to moisture loss resulting from vaporization, while the steady decline in weight between 150°C and 1,000°C, with a total loss of approximately 20%, can be attributed to decomposition and volatilization of metallic oxides and some functional groups presented in the carbon structure. With respect to raw sludge, Fig. 3(d) shows that an appreciable weight loss of approximately 48% occurred between 200°C and 600°C, which can be attributed to pyrolytic reaction occurring within this temperature range that resulted in decomposition of organic constituents presented in the raw sludge, which was followed by release of volatile compounds [1]. Pullket et al. [1] reported that decomposition of aliphatic compounds and organic acids into gaseous byproduct occurs at this temperature range. Organic compounds such as paper and cellulose present in sludge might have been the source of the sharp weight decline. At a temperature range of 600°C–1,000°C, lower rate of steady weight loss of approximately 14% was observed, which indicates that sludge is thermally stable at this temperature range. In total, a weight loss of approximately 66% was observed from the TG analysis of the raw sludge sample. The DTG curves show decomposition peaks for AC and sludge samples, which identify temperature regions at which weight loss is most clear. The curves of AC and sludge samples have similar peak type, with sharp peaks occurring close to a temperature of 100°C in all samples. A second shorter broad peak can be found around 750°C–800°C for $ZnCl_2$ AC samples, while in KOH AC sample, a short sharp peak can be observed at the same temperature range. The curves clearly show that sludge produced a considerable sharp peak at a temperature range of 750°C–800°C, which was attributed to weight change resulting from decomposition of inorganic constituents.

3.3.3. Porosity and surface area analysis

Table 7 shows surface properties of sludge and produced AC samples that were determined from nitrogen

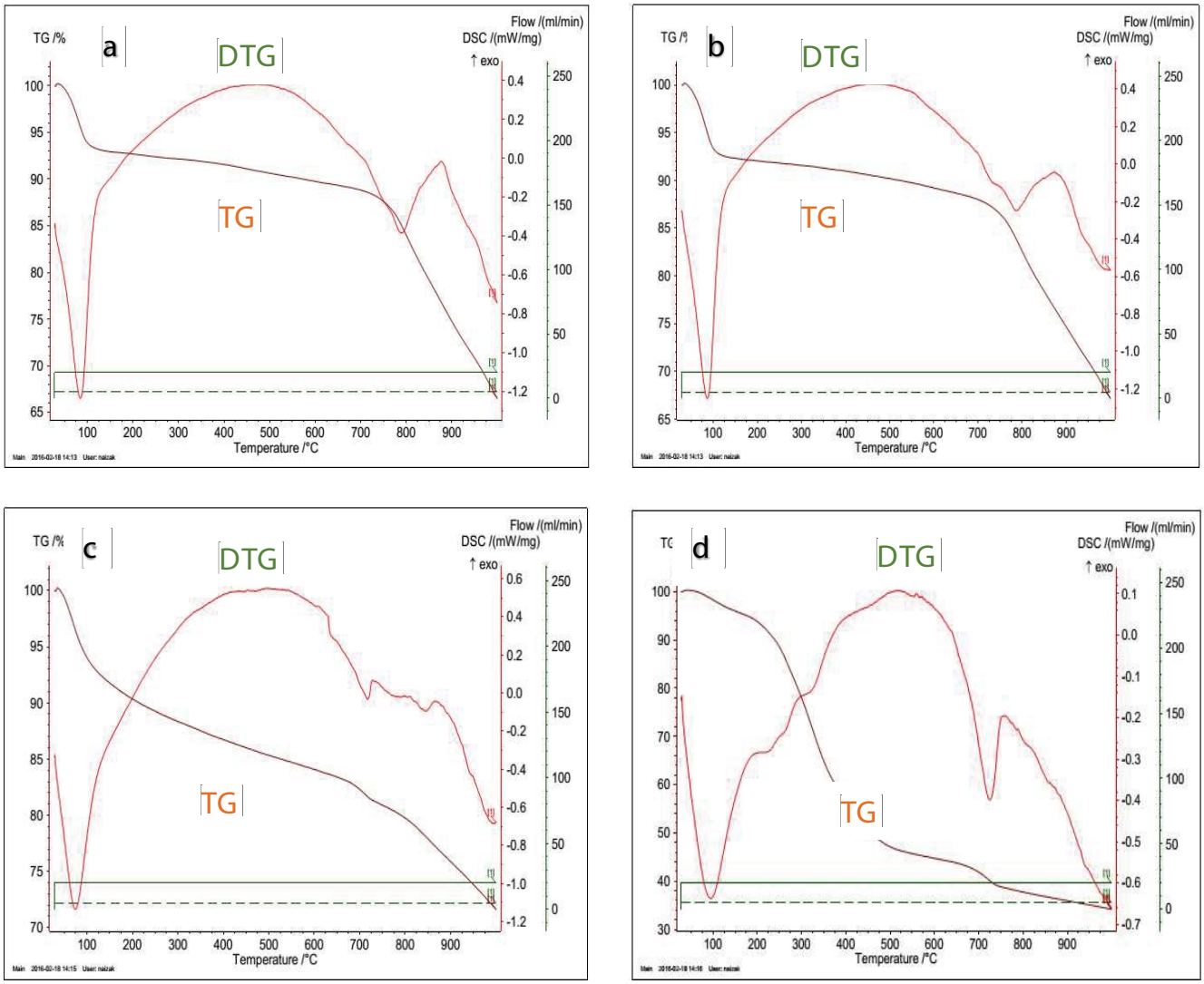

Fig. 3. TG and DTG curves of sludge and produced AC samples. (a) AC1-$ZnCl_2$; (b) AC2-$ZnCl_2$; (c) AC3-KOH; and (d) sludge.

Table 7
Specific surface area properties of sludge and produced AC samples

Sample	Activation conditions (temp./time/conc.)	SSA_{BET} total (m^2/g)	Micro pore area (m^2/g)	External area (m^2/g)	V_{total} (cm^3/g)	V_{micro} (cm^3/g)	D_p (Å)
AC1-$ZnCl_2$	700°C/120 min/5 M	314.4	101.06	213.35	0.246	0.176	31.31
AC2-$ZnCl_2$	700°C/60 min/5 M	319.5	102.45	217.04	0.249	0.0056	31.28
AC3-KOH	700°C/120 min/1:1.5	347.7	67.749	279.96	0.640	0.0364	69.51
Dried sludge	N/A	0.664	N/A	N/A	0.0127	0.0016	763.82

adsorption–desorption isotherm at 77 K using Accelerated Surface Area and Porosimetry System (ASAP) 2020 (Micromeritics) instrument. The SSA was determined using the BET method, and micropore area and volume were obtained through the *t*-plot method. The SSA_{BET} of the sludge sample was low (0.664 m^2/g), when compared with reported values in the published literature (approximately 3 m^2/g) [9,28], which was attributed primarily to characteristics of the sludge. Improvement in surface properties of sludge after chemical activation, as shown by the SSA_{BET} of the AC samples, indicates the removal of organics and inorganics present in sludge samples that resulted in improving surface properties [28]. The SSA_{BET} of the three AC samples were marginally close (around 314–348 m^2/g), which indicates that activation reagents ($ZnCl_2$ and KOH) had no significant contribution to pore development. These values were

lower than those reported in the published literature for AC produced from sewage sludge. As an example, the highest SSA_{BET} reported for sewage sludge activated using KOH (KOH: sludge ratio is 1:1) was 1,882 m^2/g that was achieved by Lillo-Rodenas et al. [23] in their two-stage activation method, where sludge was carbonized (first stage) before being impregnated and activated (second stage). Moreover, Xu et al. [10] who reviewed SBAs reported that the highest SSA_{BET} achieved from $ZnCl_2$ activation of sewage sludge was 757 m^2/g. The relatively low SSA_{BET} values achieved in the current research is most likely due to the nonmicroporous nature of the produced AC samples. However, Sheha et al. [29] reported a BET surface area of 187.5–307 m^2/g for sludge activated with $ZnCl_2$. Pore sizes of produced AC samples were found to be in the range of 3–7 nm and, consequently, it can be concluded that the activation process, under investigation, created mesoporous AC structures, where mesopore diameters are between 2 and 50 nm. Similar results were also reported by Gupta and Garg [28], who investigated the production of AC from sewage sludge using KOH and $ZnCl_2$. Although, their reported SSA_{BET} (495–515 m^2/g) was higher than those achieved in this study, the difference could be attributed to the production method employed, where the pyrolysis was not performed in an inert environment but in low oxygen environment. Moreover, the disparity might be due to the low organic contents of sludge used in the current study, as was shown in the elemental analysis.

3.3.4. Surface morphology

Fig. 4 shows SEM micrographs of surface morphology of sludge and AC samples. The figure clearly shows that micrograph (a), which was taken for sludge without activation, shows a compact sample with no sign of visible pores

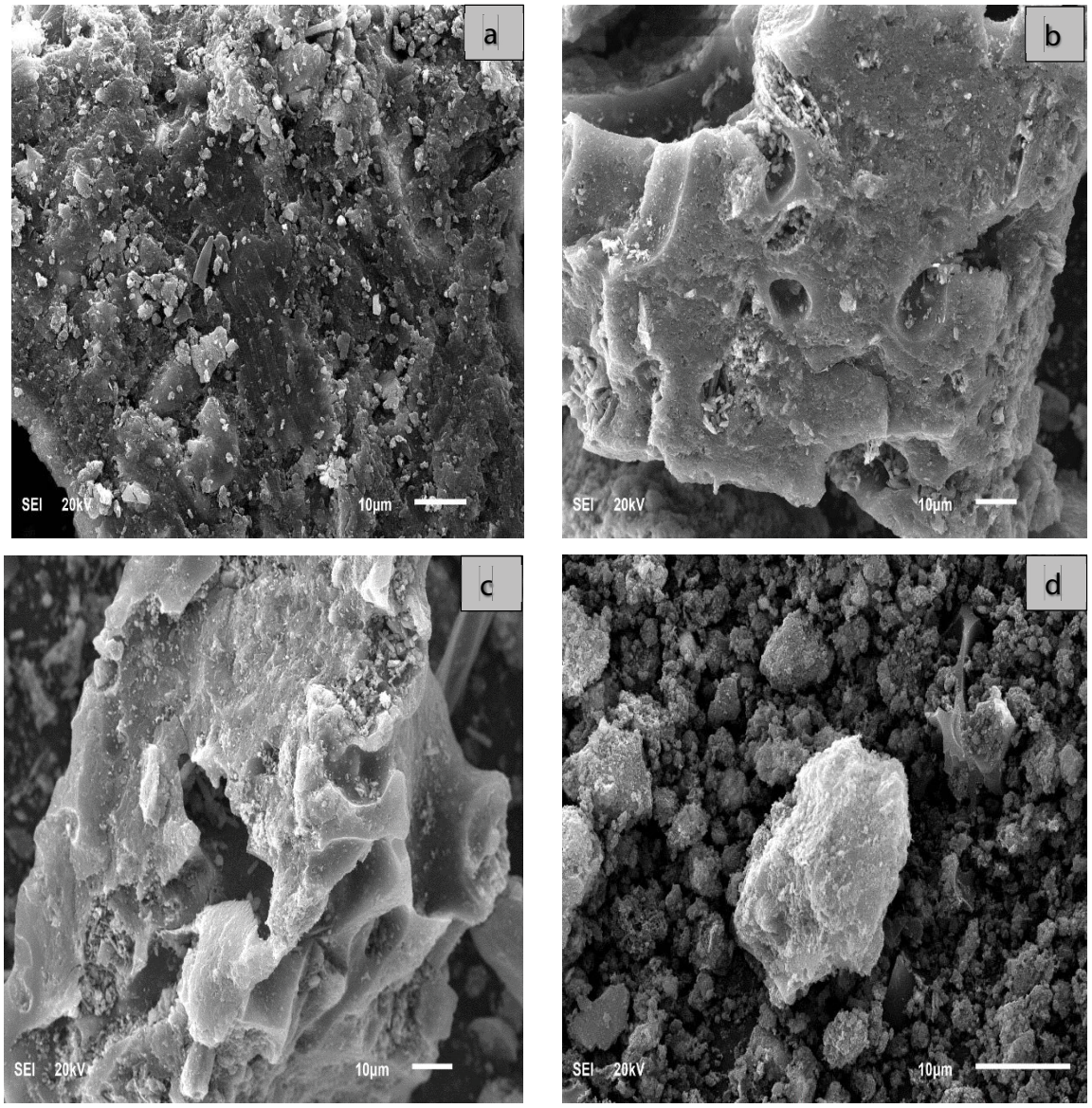

Fig. 4. SEM image of (a) sludge, (b) AC1-$ZnCl_2$, (c) AC2-$ZnCl_2$, and (d) AC3-KOH.

that supports the low S_{BET} (0.664 m^2/g) obtained for sludge. However, when sludge was activated using $ZnCl_2$ and KOH, dramatic improvements were observed, as shown in micrographs (b)–(d) that were taken for samples AC1-$ZnCl_2$, AC2-$ZnCl_2$, and AC3-KOH, respectively. When comparing micrographs of $ZnCl_2$ AC samples with those of KOH, few cavities and pore structures can be clearly seen in AC1-$ZnCl_2$ and AC2- $ZnCl_2$, with no sign of pores in AC3-KOH. These results explain why the $ZnCl_2$ AC samples have more micropore surface area than that of the KOH, in spite of the fact that KOH AC sample presented the highest total surface area, as obtained from the BET analysis results. Formation of cavities and pores in $ZnCl_2$ AC samples might have resulted from the decomposition of $ZnCl_2$ during the carbonization process [30]. Additionally, the washing step might have assisted in making those pores more visible through the removal of trapped $ZnCl_2$ and ZnO [8]. As for AC3-KOH, the effect of activation process has resulted in increasing its surface roughness, as demonstrated by the SEM micrograph, as well as increasing its external surface area. Similar findings were reported by dos Reis et al. [31], who produced AC from sewage sludge.

3.3.5. X-ray diffraction spectroscopy

Fig. 5 shows XRD patterns of sludge and produced AC samples, which displays the appearance of several sharp peaks in all the samples that confirms the presence of crystalline minerals in all samples. The sludge XRD pattern shows several sharp peaks that were identified to be due to the presence of calcite, dolomite, carbon, and quartz. Zinc silicate mineral (Willemite) was observed to be dominant in $ZnCl_2$ AC samples (AC1-$ZnCl_2$ and AC2-$ZnCl_2$), which might have resulted from the reaction of quartz (SiO_2) present in the sludge with the $ZnCl_2$. The figure shows that AC1-$ZnCl_2$ and AC2-$ZnCl_2$ share similar XRD patterns, except for the graphite (carbon) peak that appeared to be lower in AC1-$ZnCl_2$, which was attributed to the high carbonization time that was employed (120 min). Moreover, the presence of Hematite (Fe_2O_3) in both AC1-$ZnCl_2$ and AC2-$ZnCl_2$ samples might have resulted from the iron tubes that were used during the carbonization process. The diffraction pattern of AC3-KOH shows the presence of calcite, graphite, and quartz. The figure clearly shows that the calcite peak in AC3-KOH was lower than that of sewage sludge, which might have been due to the decomposition of calcite ($CaCO_3$) into calcium oxide (CaO) at high temperatures. Ahmad and Idris [9] reported similar results in their review paper on SBAs. Results of the XRF analysis also confirm the presence of a relatively high percentage of calcium oxide in AC3-KOH.

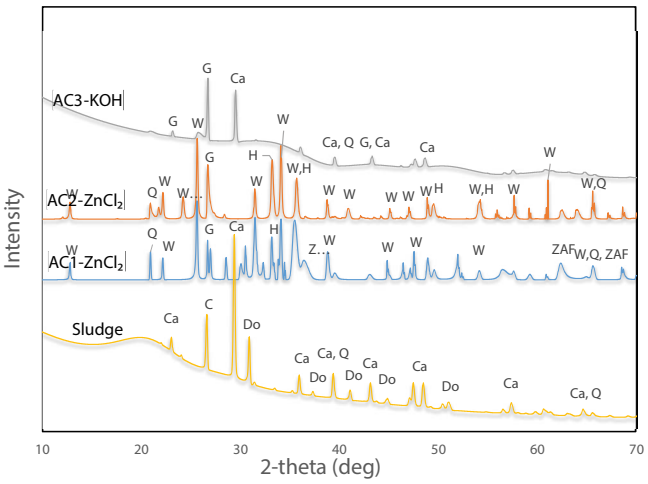

Legend		
W	Willemite	Zn_2SiO_4
Ca	Calcite	$CaCO_3$
C	Carbon	C
G	Graphite	C
Do	Dolomite	$CaMg(CO_3)_2$
Q	Quartz	SiO_3
H	Hematite	Fe_2O_3
ZAF	Zinc Aluminum Iron Oxide	$Al_2FeO_2O_4ZnO_8$

Fig. 5. XRD patterns of sludge and produced AC samples.

3.3.6. X-ray fluorescence analysis

Table 8 shows the XRF results of sludge and produced AC samples, which demonstrates the percent concentrations of elements oxides present in samples. Major oxides identified in sludge samples were calcium oxide, iron(III) oxide, and silica, which are 36%, 13%, and 8%, respectively. Similar proportions of these oxides but with a slight increase can also be seen in the AC3-KOH, which can be attributed

Table 8
XRF analysis of sludge and produced AC samples

Concentration (%)	Symbols	AC1-$ZnCl_2$	AC2-$ZnCl_2$	AC3-KOH	Sludge
Aluminum	Al_2O_3	2.208	2.354	4.710	3.606
Silicon	SiO_2	4.672	4.651	12.41	8.387
Phosphorus	P_2O_5	5.090	5.089	10.07	7.819
Sulfur	S	1.552	1.651	0.4405	5.098
Chlorine	Cl	2.845	3.035	0.2411	0.815
Potassium	K_2O	0.04734	0.04302	1.668	1.106
Calcium	CaO	9.479	10.85	39.29	35.78
Chromium	Cr_2O_3	3.13	3.146	0.7051	0.1529
Iron	Fe_2O_3	39.32	34.93	15.46	12.60
Zinc	ZnO	24.76	27.89	3.605	2.721

to concentrations of inorganic constituents of sludge during carbonization process, where organics volatilized. Similar observations were reported by Ros et al. [32] in their research work, where they observed that concentrations of inorganic minerals in char of sewage sludge (pyrolyzed sludge) tend to double after thermal treatment. As expected, concentration of potassium oxide (K_2O) in AC3-KOH was more when compared with those of sludge and produced AC samples. Also, percent concentrations of zinc oxide (ZnO) in AC1-$ZnCl_2$ and AC2-$ZnCl_2$ were also found to be higher, which must have resulted from activation with $ZnCl_2$.

3.3.7. Fourier transform infrared analysis

FTIR spectra of sludge and produced AC samples are presented in Fig. 6, which shows the broad bands appearing in the range of 3,700–3,200 cm^{-1} for all samples, which can be attributed to the presence of free O–H functional group or N–H amides group. The N–H amides group is most likely to present in sludge, as it could result from the presence of protein structure [1]. The appearance of strong intensity band at this range for AC3-KOH could indicate the presence of significant O–H functional group, which might have been due to its activation with KOH. The bands at 2,924.6 and 2,851.3 cm^{-1} for sludge spectra was attributed to C–H stretching of aliphatic hydrocarbon structure, which can be associated with the glicydic part of lipids [10,12]. These two bands were absent in AC samples and could have been due to lipid removal during the pyrolysis stage. Strong bands at 1,666.1 and 1,636.8 cm^{-1} for sludge and AC3-KOH samples, respectively, were assigned to C=O (carbonyl group) stretching in primary amide, which also supports the presence of lipids in sludge [9]. Moreover, the band at 1,540.9 for sludge was attributed to N–H stretching in primary amides, confirming the presence of protein structure in sludge [33]. In addition, the band at 1,412.7 cm^{-1} for sludge and 1,388.3 cm^{-1} for AC3-KOH were assigned to the presence of organic sulfate, where similar band was reported by Ros et al. [32], who investigated AC production from sewage sludge. The figure also shows that AC1-$ZnCl_2$ and AC2-$ZnCl_2$ samples have weak bands at 1,100.7 and 1,043.5 cm^{-1}, respectively, which can be attributed to the presence of carboxyl group (C–O stretching). Similarly, the band at 1,591.8 cm^{-1} for both samples was associated with the presence of C–C stretching of aromatic group. The presence of inorganic compounds in sludge is noticeable in strong bands appearing at 1,030.5 cm^{-1} and other weak bands at 463.0, 443.6, and 432.3 cm^{-1}, which were all assigned to silica ion Si–O–Si bending that resulted from the presence of quartz or feldspar [1]. These same sets of bands were also found in AC3-KOH, but with a stronger band at 1,031.1 cm^{-1}, signifying the presence of significant amount of silica. The XRF analysis also confirms the presence of a relatively high percentage of silica in AC3-KOH. The silica ion band was also found in AC1-$ZnCl_2$ and AC2-$ZnCl_2$ at bands 463.0, 443.6, 432.3 and 461.0, 443.4, 420.4 cm^{-1}, respectively. With respect to inorganic constituents, sharp bands at 871.1, 871.3, 862.2, and 864.1 cm^{-1} for sludge, AC1-$ZnCl_2$, AC2-$ZnCl_2$, and AC3-KOH, respectively, were assigned to the presence of calcite [10,12], which support XRD and XRF results that indicated the presence of calcite in all samples. Another notable inorganic compound that was identified in all samples was phosphate, which appeared in the form of PO_4^{3-} bending, and was noticeable in the band region of 500–600 cm^{-1}. When comparing the spectra of sludge with those

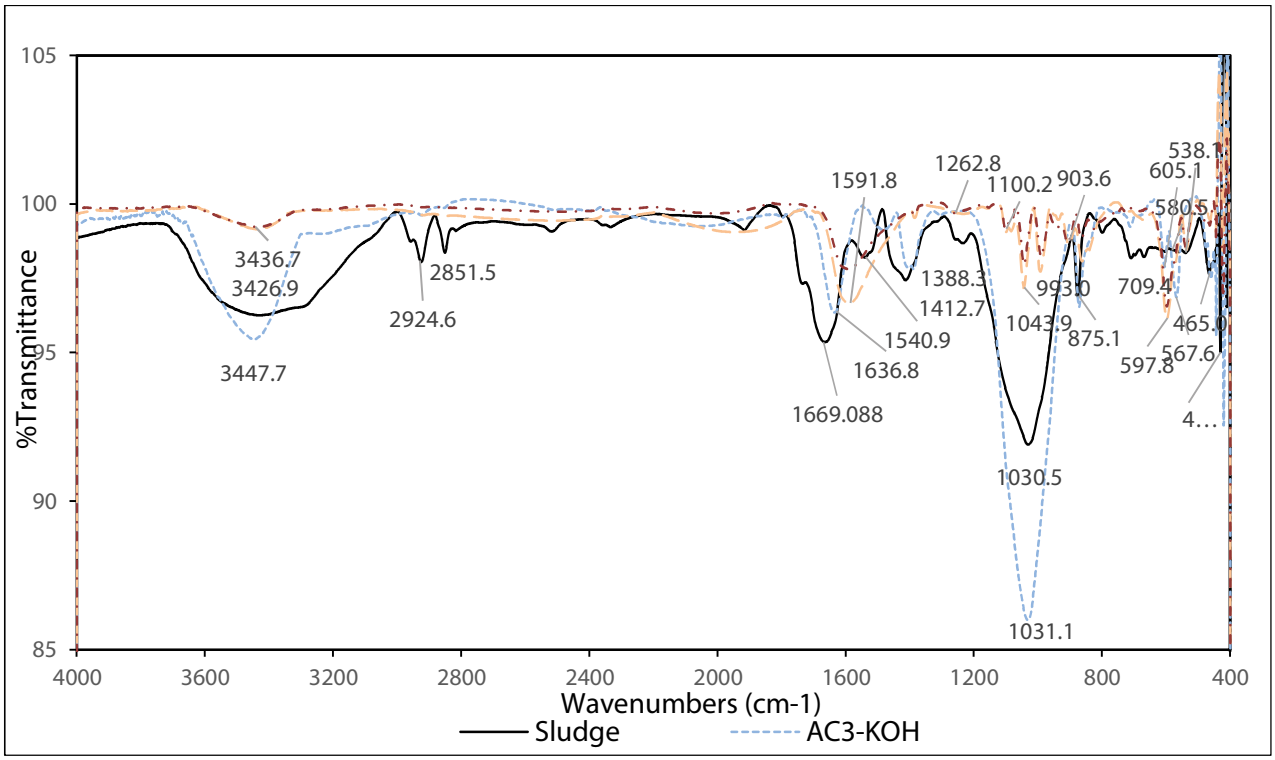

Fig. 6. FTIR spectra of sludge and produced AC samples.

of produced AC samples, it can be deduced that conversion of sludge to AC through carbonization and chemical impregnation processes brought about an improvement in surface properties, where new functional groups were observed in AC samples. In summary, functional groups identified in AC samples were O–H, C–C, C–O, and C=O. It is worth to mention that the presence of these groups on AC surface has been reported to be highly effective for heavy metals and toxic organics uptake [34–35].

4. Conclusions and recommendations

Sewage sludge was used as a precursor to produce low-cost AC, where several AC samples were produced through chemical activation method using three activation agents, namely $ZnCl_2$, H_3PO_4, and KOH. The production process was designed and optimized using RSM and BBD techniques. Effects of chemical impregnation ratio and activation temperature and time on the production process were investigated using two responses, which were MB removal efficiency and yield of AC samples. Consequently, three quadratic models were formulated and significant and insignificant models and terms were presented. Moreover, based on the results of the production process and statistical analysis of the response data, three AC samples that were produced using $ZnCl_2$ and KOH, were selected for the characterization study. The selected samples were characterized using several techniques such as FTIR, SEM, XRD, elemental analysis, TGA, porosity, and surface area analysis. The results showed that the best AC sample that was produced using $ZnCl_2$ as the activation agent had a specific BET surface area of 319.5 m^2/g and was produced at activation temperature of 700°C, impregnation ratio of 1:0.6 (sludge: reagents) and activation time of 60 min. Dominant functional groups presented on the surfaces of the produced AC samples were O–H, C–C, C–O, and C=O. In order to improve the production process, it is highly recommended that incorporation of inert gas should be implemented in the carbonization process to reduce high rates of carbon burning that was witnessed in the current investigation, which can help in improving surface properties and yields of the produced AC samples. Moreover, other carbonization methods such as hydrothermal carbonization, microwave carbonization can be explored. Furthermore, the use of other activation agents such as H_2SO_4, K_2CO_3, and HNO_3 can be studied in order to obtain high-performance AC with improved surface properties and pore structures.

Acknowledgment

The authors would like to thank King Fahd University of Petroleum & Minerals (KFUPM, Dhahran, Saudi Arabia) for their technical and financial supports.

References

[1] S. Pullket, Sewage sludge as source of activated carbon for the removal of endocrine disrupting chemicals in wastewater, PhD Dissertation, Imperial College, London, 2015.
[2] F. Çeçen, Ö. Aktaş, Fundamentals of Adsorption onto Activated Carbon in Water and Wastewater Treatment, Wiley-VCH Verlag GmbH & Co., Weinheim, Germany, 2011, pp. 13–41.
[3] M.A. Yahya, Z. Al-Qodah, C.W.Z. Ngah, Agricultural bio-waste materials as potential sustainable precursors used for activated carbon production: a review, Renew. Sustain. Energy Rev., 46 (2015) 218–235.
[4] M.H. Al-Malack, A.A. Basaleh, Adsorption of heavy metals using activated carbon produced from municipal organic solid waste, Desal. Wat. Treat., 57 (2016) 24519–24531.
[5] E. Kacan, Optimum BET surface areas for activated carbon produced from textile sewage sludges and its application as dye removal, J. Environ. Manage., 166 (2016) 116–123.
[6] Y. Li, Y. Li, L. Li, X. Shi, Z. Wang, Preparation and analysis of activated carbon from sewage sludge and corn stalk, Adv. Powder Technol., 27 (2015) 684–691.
[7] X. Li, W. Li, G. Wang, P. Wang, X. Gong, Preparation, characterization, and application of sludge with additive scrap iron-based activated carbons, Desal. Wat. Treat., 54 (2015) 1194–1203.
[8] K.M. Smith, G.D. Fowler, S. Pullket, N.J.D. Graham, Sewage sludge-based adsorbents: a review of their production, properties and use in water treatment applications, Water Res., 43 (2009) 2569–2594.
[9] A.A. Ahmad, A. Idris, Preparation and characterization of activated carbons derived from bio-solid: a review, Desal. Wat. Treat., 52 (2014) 4848–4862.
[10] G. Xu, X. Yang, L. Spinosa, Development of sludge-based adsorbents: preparation, characterization, utilization and its feasibility assessment, J. Environ. Manage., 151 (2015) 221–232.
[11] F.N. Kemmer, R.S. Robertson, R.D. Mattix, US Patent 3,619,420, 1971.
[12] P. Hadi, M. Xu, C. Ning, C. Sze, K. Lin, G. Mckay, A critical review on preparation, characterization and utilization of sludge-derived activated carbons for wastewater treatment, Chem. Eng. J., 260 (2015) 895–906.
[13] X. Wang, N. Zhu, B. Yin, Preparation of sludge-based activated carbon and its application in dye wastewater treatment, J. Hazard. Mater., 153 (2008) 22–27.
[14] Q. Wen, C. Lia, Z. Caia, W. Zhanga, H. Gaoa, L. Chena, G. Zenga, X. Shua, Y. Zhaoa, Study on activated carbon derived from sewage sludge for adsorption of gaseous formaldehyde, Bioresour. Technol., 102 (2011) 942–947.
[15] J. Alvarez, G. Lopez, M. Amutio, J. Bilbao, M. Olazar, Preparation of adsorbents from sewage sludge pyrolytic char by carbon dioxide activation, Process Saf. Environ. Prot., 3 (2016) 76–86.
[16] M.H. Al-Malack, N.S. Abuzaid, A.A. Bukhari, Physico-chemical characteristics of municipal sludge produced at three major cities of the Eastern Province of Saudi Arabia, J. King Saud Univ., 20 (2008) 15–27.
[17] M.A. Bezerra, R.E. Santelli, E.P. Oliveira, L.S. Villar, L.A. Escaleira, Response surface methodology (RSM) as a tool for optimization in analytical chemistry, Talanta, 76 (2008) 965–977.
[18] C.J. Durán-Valle, Techniques Employed in the Physicochemical Characterization of Activated Carbons, V.H. Montoya, Ed., Lignocellulosic Precursors Used in the Synthesis of Activated Carbon – Characterization Techniques and Applications in the Wastewater Treatment, InTech Open-Access Books, 2012, pp. 37–55.
[19] B.K. Körbahti, Optimization of Electrochemical Oxidation of Textile Dye Wastewater Using Response Surface Methodology (RSM), H. Gökçekus, U. Türker, J.W. LaMoreaux, Eds., Survival and Sustainability, Part of the Series Environmental Earth Sciences, Springer-Verlag Berlin Heidelberg, Germany, 2010, pp. 1181–1191.
[20] S. Uçar, M. Erdem, T. Tay, S. Karagöz, Preparation and characterization of activated carbon produced from pomegranate seeds by $ZnCl_2$ activation, Appl. Surf. Sci., 255 (2009) 8890–8896.
[21] S. Pullket, K.M. Smith, G.D. Fowler, N.J.D. Graham, Influence of source and treatment method on the properties of activated carbons produced from sewage sludge, J. Residuals Sci. Technol., 6 (2009) 43–50.
[22] T.S. Hui, M. Abbas, A. Zaini, Potassium hydroxide activation of activated carbon: a commentary, Carbon Lett., 16 (2015) 275–280.

[23] M.A. Lillo-Ródenas, A. Ros, E. Fuente, M.A. Montes-Morán, M.J. Martin, A. Linares-Solano, Further insights into the activation process of sewage sludge-based precursors by alkaline hydroxides, Chem. Eng. J., 142 (2008) 168–174.
[24] F. Zhang, H. Itoh, J.O. Nriagu, Activated carbons derived from organic sewage sludge for the removal of mercury from aqueous solution, H. Itoh, Ed., Waste Management in Japan, WIT Press, Southampton, ISBN 1-84564-000-4, 2004.
[25] H.D. Utomo, X.C. Ong, S.M.S. Lim, G.C.B. Ong, P. Li, Thermally processed sewage sludge for methylene blue uptake, Int. Biodeterior. Biodegrad., 85 (2013) 460–465.
[26] J.A. Arcibar-Orozco, J.R. Rangel-Mendez, P.E. Diaz-Flores, Simultaneous adsorption of Pb(Ii)-Cd(Ii), Pb(Ii)-phenol, and Cd(Ii)-phenol by activated carbon cloth in aqueous solution, Water, Air, Soil Pollut., 226 (2014) 1–10.
[27] C. Li, S. Kumar, Preparation of activated carbon from un-hydrolyzed biomass residue, Biomass Convers. Biorefin., 6 (2016) 407–419.
[28] A. Gupta, A. Garg, Primary sewage sludge-derived activated carbon: characterisation and application in wastewater treatment, Clean Technol. Environ. Policy, 17 (2015) 1619–1631.
[29] D. Sheha, H. Khalaf, N. Daghestani, Experimental design methodology for the preparation of activated carbon from sewage sludge by chemical activation process, Arabian J. Sci. Eng., 38 (2013) 2941–2951.
[30] İ. Demiral, C. Aydın Şamdan, H. Demiral, Production and characterization of activated carbons from pumpkin seed shell by chemical activation with $ZnCl_2$, Desal. Wat. Treat., 3994 (2015) 1–9.
[31] G.S. dos Reis, M.A. Adebayo, E.C. Lima, C.H. Sampaio, L.D.T. Prola, Activated carbon from sewage sludge for preconcentration of copper, Anal. Lett., 49 (2016) 541–555.
[32] A. Ros, M.A. Lillo-Ródenas, E. Fuente, M.A. Montes-Morán, M.J. Martín, A. Linares-Solano, High surface area materials prepared from sewage sludge-based precursors, Chemosphere, 65 (2006) 132–140.
[33] P. Fang, C. Cen, D. Chen, Z. Tang, Carbonaceous adsorbents prepared from sewage sludge and its application for Hg0 adsorption in simulated flue gas, Chin. J. Chem. Eng., 18 (2010) 231–238.
[34] K. Pirzadeh, A.A. Ghoreyshi, Phenol removal from aqueous phase by adsorption on activated carbon prepared from paper mill sludge, Desal. Wat. Treat., 52 (2014) 37–41.
[35] Y. Bian, Z. Bian, J. Zhang, Adsorption of cadmium ions from aqueous solutions by activated carbon with oxygen-containing functional groups, Chin. J. Chem. Eng., 23 (2015) 1705–1711.